

Nanotube micro-optomechanical actuators

Shaoxin Lu and Balaji Panchapakesan^{a)}

Department of Electrical and Computer Engineering, University of Delaware, Newark, Delaware 19716

(Received 27 January 2006; accepted 4 May 2006; published online 21 June 2006)

In this letter we demonstrate a simple carbon nanotube patterning technique that combines nanotube film bonding, photolithography, and O₂ plasma etching. Well defined carbon nanotube film structures with line widths less than $\sim 1.5 \mu\text{m}$ and thickness ranging from 40 to 780 nm were readily fabricated. A micro-optomechanical actuator based on this process has been demonstrated. This patterning process can be utilized for the integration of nanomaterials for wide variety of devices including microelectromechanical systems, field emission displays, and micro-optomechanical systems (MOMS). © 2006 American Institute of Physics.
[DOI: 10.1063/1.2214148]

Carbon nanotube films (CNFs) have attracted increasing interest in recent years due to their promising potentials in many applications such as field emission displays,¹ chemical sensors,^{2,3} strain sensors,⁴ thin film transistors,⁵ photodetectors,⁶ and transparent electrodes for optoelectronic devices.^{7,8} While nanotubes have been processed into macroscopic sheets and films, devices based on nanotube films employing batch fabrication techniques have been elusive. The lack of precise control of nanotube film pattern in micro- and nanoscales has become one of the major stumbling blocks for fulfilling these applications. The requirement of high quality and high resolution patterning of nanotube films into various features at desired locations on specified substrates calls for advances in nanotube patterning techniques. Pregrowth patterning such as chemical vapor deposition (CVD) was used to grow carbon nanotubes selectively onto prepatterned catalyst blocks by CVD process.^{9,10} However, it suffers from low material purity and high processing temperatures and is incompatible with complementary metal oxide semiconductor (CMOS) and microelectromechanical system (MEMS) processing. To overcome these problems, postgrowth patterning techniques such as electrophoresis deposition,^{11,12} screen printing processes,¹³ self-assembly,¹⁴ and chemically anchored deposition¹⁵ have also been explored, in which carbon nanotubes are patterned onto substrates after the growth and purification processes. However, these methods either only offer low feature resolutions or have limitations of substrate restriction, requirement of substrate modification, use of electrical field gradients, or tedious thickness control processes.

In this letter we present a simple yet versatile subtractive patterning technique, in which uniform thin nanotube films of desired thickness were formed by vacuum filtration. Then it was transferred to a substrate, followed by photolithography to define features. O₂ plasma etching was subsequently employed to selectively remove the exposed carbon nanotubes forming patterns. This method offer several advantages compared to other patterning techniques: (1) the uniformity and reproducibility of CNF (Ref. 8) within the patterns; (2) low processing temperatures compatible with polymeric substrates; (3) high feature resolutions even smaller than nanotube length due to the ability of plasma to etch the nanotubes

precisely; (4) sharp pattern edges; and (5) compatibility with MEMS fabrication technologies. As one of the applications of this patterning technique, a CNF/SU8 micro-optomechanical system (MOMS) was demonstrated, which showed elastic light induced actuation.

Commercially obtained single wall carbon nanotubes were dispersed in isopropyl alcohol to $\sim 0.1 \text{ mg/ml}$ by ultrasonication and was vacuum filtered through mixed cellulose ester (MCE) filter to produce CNFs. A simple procedure described by Zhang *et al.* was employed to transfer CNF onto silicon substrate,⁸ as shown in Fig. 1, sequences (a) to (c). Briefly, the wet CNF still on top of MCE filter was located onto silicon substrate by compressive loading. Upon CNF drying and subsequent annealing on 75 °C hot plate for 20 min, CNF sticks onto the substrate with enough adhesion strength for further processing. Then the MCE filter was dissolved in multibaths of acetone, leaving clean uniform wrinkleless CNF on the substrate after drying. Figure 2(a) shows a uniform CNF of $\sim 1 \text{ cm} \times 1 \text{ cm} \times 230 \text{ nm}^3$ transferred onto a silicon wafer. The thicknesses of CNF was well controlled by the amount of carbon nanotube solution of known concentration during vacuum filtration. Several CNFs of thickness $\sim 40, 130, 230, 460,$ and 780 nm were fabricated with high film uniformity offered by vacuum filtration process.⁸ As the film thickness was smaller than 230 nm, the

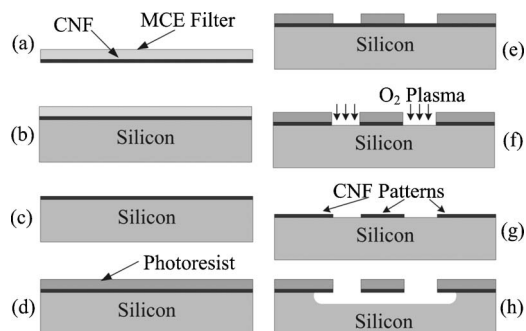


FIG. 1. The sequence of CNF transferring to substrate and subsequent patterning by plasma etching. (a) CNF on MCE filter after vacuum filtration; (b) CNF with MCE filter being transferred onto silicon substrate; (c) MCE filter dissolved; (d) spin coating photoresist; (e) photolithography; (f) O₂ plasma etching of CNF; (g) masking photoresist removed; and (h) in the case of CNF/SU8 actuator, XeF₂ etching was used to release the actuator structure.

^{a)}Electronic mail: baloo@mail.eecis.udel.edu

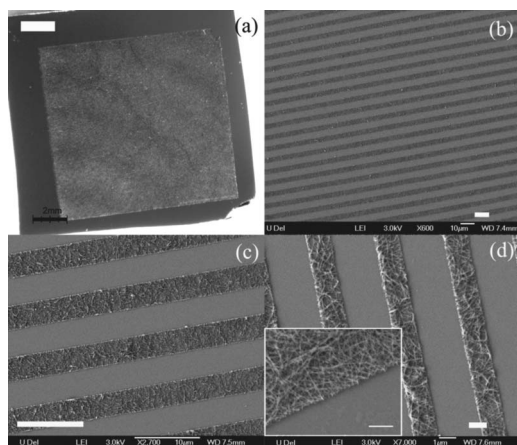


FIG. 2. (a) A semitransparent CNF of ~ 130 nm covered on silicon wafer; (b) scanning electron microscopy (SEM) image of CNF lines ~ 4 μm in width fabricated by oxygen plasma etching; (c) higher magnification image of patterns in (b); and (d) clear patterns of ~ 1.5 μm CNF lines with ~ 2 μm spacing. Inset: Sharp pattern edge formed by nanotube cutting in O_2 plasma. Scale bars: (a) 2 mm, [(b) and (c)] 10 μm , (d) 1 μm , and insert in (d), 500 nm.

CNF showed a high degree of transparency visible to naked eyes.

Photolithography was then employed to define CNF patterns on the substrate. Several commercial photoresists of both positive and negative tones, including AZ5214E, NR7-1500, AZ4620, and SU8, have been tested and all formed excellent features on top of CNF. This indicates that randomly oriented nanotubes packed into thin films hardly affect the lithographic process. The excellent compatibility of CNF with photolithography offered the opportunity of defining precise and high resolution features onto CNF through lithography, with virtually only one requirement being the photoresist thickness. Since O_2 plasma attack photoresists, the etch mask out of photoresist needs to be thick enough to sustain continuous O_2 plasma etching. For CNF with thickness smaller than 460 nm, ~ 1.5 μm photoresist (AZ5214E) was used as the etch mask. Commercial thick film photoresists such as AZ4620 was also used to pattern thick etch masks up to tens of microns for etching thicker CNFs. Sequences (d) and (e) in Fig. 1 illustrated the photolithography processes.

O_2 plasma has been widely used to remove carbon based organic materials such as photoresists from substrate surfaces. It forms volatile CO , CO_2 , and H_2O which can be pumped out from the system during plasma etching.¹⁶ However, the O_2 plasma etching of carbon nanotubes to define prepatterned films has not been reported until now. By employing a similar idea, we used O_2 plasma in inductively coupled plasma (ICP) system to etch the carbon nanotubes in order to form CNF patterns. Surprisingly, at ICP power ~ 200 W, bias power ~ 100 W, and O_2 flow rate ~ 50 SCCM (standard cubic centimeter per minute), an etch rate of CNF at ~ 4 nm/s was achieved, showing the fast etching of carbon nanotubes in strong O_2 plasma. Carbon nanotubes are well known for their chemical resistance and high stability.¹⁷ However, structural defects are often present in real carbon nanotube samples, especially after purification and ultrasonic dispersion steps.¹⁸ At the same time, defects could also form on carbon nanotubes under bombardments of high energy species in plasma ambient.¹⁹ It is possible that

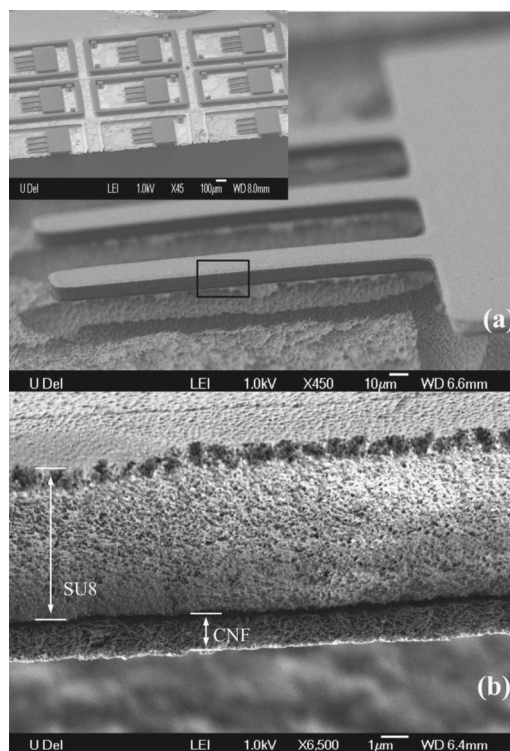


FIG. 3. (a) SEM image of released CNF/SU8 actuators. Inset: SEM image of a $3 \times 3 \times 3$ actuator arrays. (b) SEM image of the squared region in (a) showing the bilayer cross section of the actuator.

the oxygen plasma reacts with the carbon nanotubes starting from these defects, consuming the whole nanotubes gradually. After etching, mild acetone rinsing served to dissolve the etch mask to leave clean CNF patterns. The etching process and subsequent etch-mask removal was schematically shown in Figs. 1(f) and 1(g). Well defined CNF stripe lines of ~ 4 μm in width and 130 nm in thickness were fabricated with all the unwanted CNF removed, as shown in Figs. 2(b) and 2(c). The clear patterns showed the effectiveness of CNF patterning through O_2 plasma etching. In Fig. 2(d), CNF lines as small as ~ 1.5 μm were also routinely produced on 130 nm thick CNF, with well defined shapes and sharp feature edges. Moreover, we believe that higher resolution patterns with feature sizes even smaller than nanotube lengths are still possible to achieve because of the ability of O_2 plasma to "cut" exposed carbon nanotubes to leave sharp pattern edges, as witnessed in the insert of Fig. 2(d). Electron beam lithography can reduce the size of CNF patterns, potentially achieving feature size in the sub-100-nm regime for nanotube devices. The reason for such excellent pattern transfer may also be due to the lack of stresses in the nanotube films after vacuum filtration, which is important in most surface microfabrication technologies.

The excellent processibility of CNF offered by O_2 plasma etching could lead to many potential applications. As one example, nanotube based MOMS actuators were fabricated to realize optical actuation. SU8 photoresist, which has excellent mechanical properties, large thermal expansion coefficient, and biocompatibility, was used in lithography to define the CNF features and act as etch mask in plasma etching.^{20,21} A CNF/SU8 composite structure was produced after etching, which was released from the silicon substrate by isotropic silicon etching in a homemade pulse mode XeF_2 dry etching system,²¹ as illustrated in Fig. 1, sequence (h). A

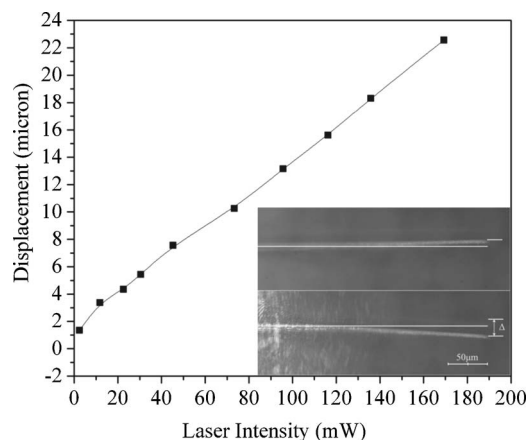


FIG. 4. The displacement of the CNF/SU8 actuator as a function of the laser intensity. Insert: Cross-sectional view of actuation under laser light stimulus. Straight lines were drawn for eye guidance.

blind cut of the substrate after actuator release also helped to get a better view of actuation from this cantilever actuator. Arrays of actuators were shown in the insert of Fig. 3(a). The magnified image of $\sim 30 \mu\text{m}$ (width) $\times 300 \mu\text{m}$ (length) $\times 7 \mu\text{m}$ (thickness) cantilevers after releasing were also shown in Fig. 3(a). Figure 3(b) showed the cross-sectional area of the cantilever, with the SU8 and CNF layers clearly observed. This indicates that high quality CNF layer can be formed from plasma etching and can be introduced into microdevices to exhibit multiple functionalities. When 808 nm laser light collimated into $\sim 0.5 \times 2 \text{ mm}^2$ spot was pointed to the cantilever, it actuated with bending toward the side of CNF. Figure 4 showed the cantilever bending as a function of laser power. A nearly linear response was shown with a maximum displacement of $\sim 23 \mu\text{m}$ under 170 mW illumination in air. The insert in Fig. 4 clearly showed the bending of actuator under light exposure. The performance of this MOMS actuator was comparable with that of electrically actuated SU8 actuators.^{20,21} The actuation arises due to the physical interlinks between elastic, electrostatic, optical, and thermal effects in nanotubes.²² Most MEMS based electrostatic actuators require large voltage for actuation. This MOMS actuator exhibited eye observable actuation up to 15 Hz. We believe that further refining of device structure and physical properties of nanotubes can greatly improve its actuation performance and also impart wavelength selectivity to these actuators.

In conclusion, well defined high resolution CNF patterns were achieved by the combination of nanotube film formation, transferring, photolithography, and O_2 plasma etching processes. This process offers high resolution of CNF pat-

terns and excellent reproducibility compared to conventional methods. A CNF/SU8 MOMS actuator, was realized through this technique. This technique can find wide variety of applications in MEMS, field emission displays, optical actuators, and biomedical nanotechnology for devices to study protein interactions.

Funding for this research work was partially supported by the NSF CAREER Award ECS: 0546328 for one of the authors (B.P.). The authors thank Guangchi Xuan for providing help with the XeF_2 etching.

- ¹O. Groning, O. M. Kuttel, C. Emmenegger, P. Groning, and L. Schlapbach, *J. Vac. Sci. Technol. B* **18**, 665 (2000).
- ²J. S. Oakley, H.-T. Wang, B. S. Kang, Z. Wu, F. Ren, A. G. Rinzler, and S. J. Pearton, *Nanotechnology* **16**, 2218 (2005).
- ³L. Valentini, I. Armentano, J. M. Kenny, C. Cantalini, L. Lozzi, and S. Santucci, *Appl. Phys. Lett.* **82**, 961 (2003).
- ⁴D. Prasad, L. Zhiling, N. Satish, and E. V. Barrera, *Nanotechnology* **15**, 379 (2004).
- ⁵T. Takenobu, T. Takahashi, T. Kanbara, K. Tsukagoshi, Y. Aoyagi, and Y. Iwasa, *Appl. Phys. Lett.* **88**, 033511 (2006).
- ⁶J. H. Lehman, C. Engtrakul, T. Gennett, and A. C. Dillon, *Appl. Opt.* **44**, 483 (2005).
- ⁷A. D. Pasquier, H. E. Unalan, A. Kanwal, S. Miller, and M Chhowalla, *Appl. Phys. Lett.* **87**, 203511 (2005).
- ⁸Z. Wu, Z. Chen, X. Du, J. M. Logan, J. Sippel, M. Nikolou, K. Kamaras, J. R. Reynolds, D. B. Tanner, A. F. Hebard, and A. G. Rinzler, *Science* **305**, 1273 (2004).
- ⁹S. Fan, M. G. Chapline, N. R. Franklin, T. W. Tombler, A. M. Cassell, and H. Dai, *Science* **283**, 512 (1999).
- ¹⁰J. J. Sohn, S. Lee, Y. H. Song, S. Y. Choi, K. J. Cho, and K. S. Nam, *Appl. Phys. Lett.* **78**, 901 (2001).
- ¹¹B. Gao, G. Z. Yue, Q. Qiu, Y. Cheng, H. Shimoda, L. Fleming, and O. Zhou, *Adv. Mater. (Weinheim, Ger.)* **13**, 1770 (2001).
- ¹²W. B. Choi, Y. W. Jin, H. Y. Kim, S. J. Lee, M. J. Yun, J. H. Kang, Y. S. Choi, N. S. Park, N. S. Lee, and J. M. Kim, *Appl. Phys. Lett.* **78**, 1547 (2001).
- ¹³W. B. Choi, D. S. Chung, J. H. Kang, H. Y. Kim, Y. W. Jin, I. T. Han, Y. H. Lee, J. E. Jung, N. S. Lee, G. S. Park, and J. M. Kim, *Appl. Phys. Lett.* **75**, 3129 (1999).
- ¹⁴S. J. Oh, Y. Cheng, J. Zhang, H. Shimoda, and O. Zhou, *Appl. Phys. Lett.* **82**, 2521 (2003).
- ¹⁵M. S. Jung, Y. K. Ko, D. H. Jung, D. H. Choi, H. T. Jung, J. N. Heo, B. H. Sohn, Y. W. Jin, and J. Kim, *Appl. Phys. Lett.* **87**, 013114 (2005).
- ¹⁶M. J. Madou, *Fundamentals of Microfabrication: The Science of Miniaturization* (CRC, Boca Raton, FL, 2002).
- ¹⁷M. S. Dresselhaus, G. Dresselhaus, and P. Avouris, *Carbon Nanotubes Synthesis, Structure, Properties, and Applications* (Springer, Berlin, 2001).
- ¹⁸J. Liu, A. G. Rinzler, H. Dai, J. H. Hafner, R. K. Bradley, P. J. Boul, A. Lu, T. Iverson, K. Shelimov, C. B. Huffman, F. R. Macias, Y.-S. Shon, T. R. Lee, D. T. Colbert, and R. E. Smalley, *Science* **280**, 1253 (1998).
- ¹⁹A. Hassani, M. Tokumoto, P. Umek, D. Vrbancic, M. Mozetic, D. Mihailovic, P. Venturini, and S. Pejovnik, *Nanotechnology* **16**, 278 (2005).
- ²⁰N. T. Nguyen, S. S. Ho, and C. L. Low, *J. Micromech. Microeng.* **14**, 969 (2004).
- ²¹N. Chronis and L. P. Lee, *J. Microelectromech. Syst.* **14**, 857 (2005).
- ²²S. Lu and B. Panchapakesan, *Nanotechnology* **16**, 2548 (2005).